INTL JOURNAL OF ELECTRONICS AND TELECOMMUNICATIONS, 2018, VOL. 64, NO. 3, PP. 335–341
Manuscript received May 8, 2018; revised July, 2018. DOI: 10.24425/123527

# Optimization of the Spectrum of Digital Diagnostic Signals to Improve the Analysis of Harmonic Parameters Using Resampling Algorithms

Marcin Jarmołowicz, and Eugeniusz Kornatowski

***Abstract*—Analysis of harmonic parameters and detection of foreign frequencies in diagnostic signals, which are most often interpreted as fault results, may be problematic because of the spectral leakage effect. When the signal contains only the fundamental frequency and harmonics, it is possible to adjust its spectral resolution to eliminate any distortions for regular frequencies. The paper discusses the influence of resampling distortions on the quality of spectral resolution optimization in diagnostic signals, recorded digitally for objects in a steady state. The method effectiveness is measured with the use of a synthetic signal generated from an analog prototype whose parameters are known. In order to achieve low values of harmonic amplitude errors in the diagnostic signal, a high quality resampling algorithm should be used, therefore the analysis of distortions generated by four popular reasampling methods is performed. Errors are measured for test signals containing different spectral structures. Finally, the results of the test of the analyzed method in practical applications are presented.**

***Keywords*—digital diagnostic signals, signal resampling; spectral resampling**

## I. Introduction

THE problem with the correct analysis of harmonic parameters and detection of foreign frequencies in the signal can be illustrated by a digital signal generated from an analog prototype, containing the fundamental frequency and harmonics, some foreign frequencies and noise. Its ideal spectrum is shown in Fig. 1.

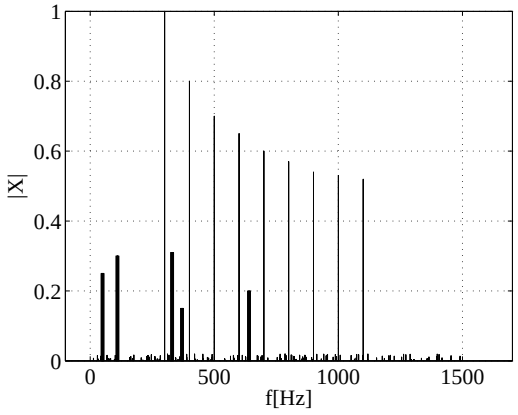


Fig. 1. The ideal spectrum of the test signal

M. Jarmołowicz and E. Kornatowski are with the West Pomeranian University of Technology, Szczecin, Poland (e-mail: marcin.jarmolowicz@zut.edu.pl, eugeniusz.kornatowski@zut.edu.pl).

Excluding noise, the signal contains the main frequencies: 300Hz, 400Hz... 1.1kHz and foreign frequencies (marked with a bold line): 50Hz, 110Hz, 330Hz, 370Hz, 640Hz. Fig. 2 shows the spectrum for the same signal computed with FFT (fast Fourier transform) for 2048 samples (sampling frequency: 44.1kHz), where a widely known effect of spectral leakage can be observed.

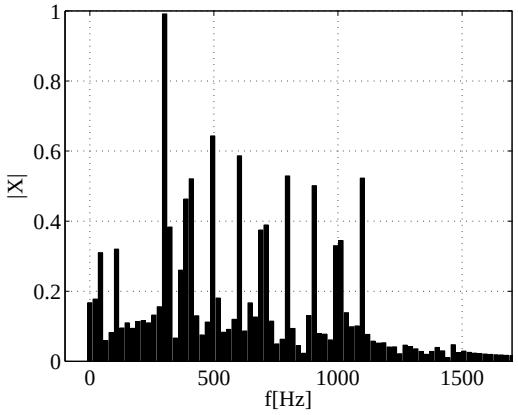


Fig. 2. Spectrum of the test signal without any optimization

As a consequence of spectral distortion:

- it is difficult to distinguish between harmonics and foreign frequencies located close to harmonics
- harmonics amplitudes are distorted
- the noise level is too low to be visible in the FFT vector

The most popular technique for reducing the spectrum leakage is to use the window functions [1]. There are a lot of windows used for this purpose, but for such signals the results are similar: the spectral leakage is significantly lower, but the harmonics are blurred and have distorted amplitudes both in absolute terms and in relation to each other (tested for Hann, Gauss, classic Blackman and Blackman-Harris windows). Therefore, the detection of foreign frequencies is still difficult. An example for the Hann window applying for the test signal is presented in Fig. 3.

Spectral resolution correctly adjusted to harmonics requires setting its value to any multiple of 100Hz. The spectrum obtained in this way almost perfectly reflects the actual harmonics structure. The foreign frequencies present in FFT vector contain the same errors as in the unoptimised FFT, which, however, does not affect the ability to detect irregularities in a

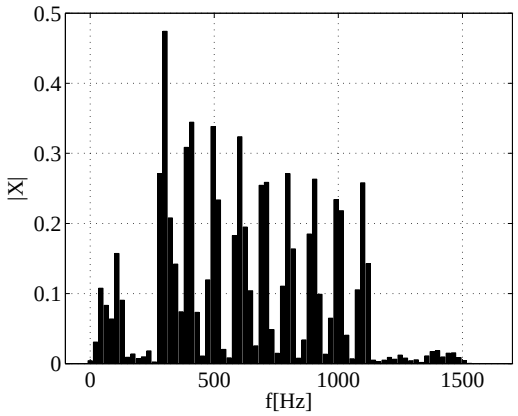


Fig. 3. The spectrum of the test signal optimized by the Hann window

negative way. For the test purpose, the spectral resolution is set to 25Hz, so for 2048 samples, upsampling will be performed with the output sampling frequency equal to 51.2kHz. The spectrum of the optimized signal is presented in Fig. 4.

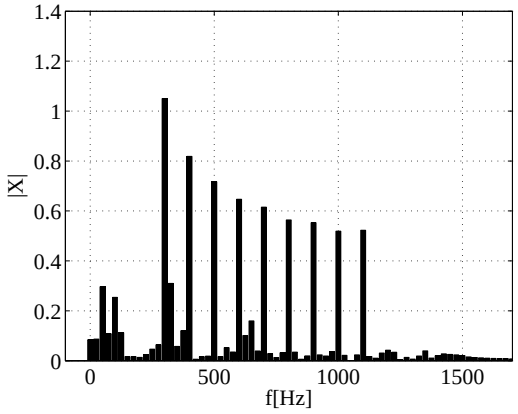


Fig. 4. The test signal spectrum optimized by adjusting spectral resolution

In practical applications, it is important to set the spectral resolution to a several times lower value than the difference between individual harmonics. This allows easy and unambiguous detection of the spectrum disorder.

## II. Algorithms Of Resampling

### A. Resampling Methods

*1) Linear Interpolation:* For this method, new samples are searched on the line between the input samples [2]. This approach is easy to implement, fast and allowing real time signal processing, but works with low quality, especially, if the signal contains high frequencies.

*2) Cascade Of DA And AD Converters:* The method is based on the cascade connection of analog-to-digital and digital-to-analog converters, working with the target sampling frequency. It is easy in hardware implementation, but generates large errors in the output signal.

*3) Resampling By Interpolation And Decimation:* This approach is based on signal decimation by an integer factor $M$ and interpolation by an integer factor $N$, using a low-pass filter [3]. The ratio of $N$ to $M$ must be equal to resampling factor. This very popular method provides good quality of processing, but also high computational complexity, which depends on the resampling factor [4].

*4) Spectral Resampling With Spectral Resolution Adjustment:* It is a high quality algorithm that [5] can be defined in the following steps:

- adding some zero-samples at the end of the input signal to obtain the same spectral resolution for the natural number of samples for both the input and the output signal. The number of new samples is given by the formula:

$$M_{in} = \frac{fs_{in}(N_{out} + M_{out})}{fs_{out}} - N_{in} \tag{1}$$

  where $fs_{in}, fs_{out}$ are original and target sampling frequency, $N_{in}, M_{in}$ are original and additional natural number of samples for input signal, $N_{out}, M_{out}$ are original and additional number of samples for output signal. $M_{out}$ is any rational number for which $N_{out} + M_{out}$ is natural, where $N_{out}$ is given by formula:

$$N_{out} = \frac{fs_{out}}{fs_{in}}(N_{in} + 1) + 1 \tag{2}$$

- computing DFT for the input signal vector.
- resizing DFT vector to obtain $N_{out} + M_{out}$ length.
- computing iDFT for resized DFT vector.
- removing the complex part of values from iDFT (time domain) vector.
- changing length of output signal to $N_{out}$ samples (rounded down).

To obtain real numbers in the time domain output signal, the imaginary part was just removed as in the case of the iDFT computed for native spectrum. If the digital signal $y_n$ is presented as a result of iDFT computed for it's spectrum:

$$y_n = \sum_{k=0}^{N-1}[(\frac{1}{N}\sum_{m=0}^{N-1} y_m \cdot e^{\frac{-i\cdot 2\pi\cdot k\cdot m}{N}}) \cdot e^{\frac{-i\cdot 2\pi\cdot k\cdot n}{N}}] \tag{3}$$

where $N$ is number of samples of $y_n$, then defining:

$$A(n,m) = \sum_{k=0}^{N-1} \cos\frac{2\pi\cdot k(n-m)}{N} \tag{4}$$

and

$$B(n,m) = \sum_{k=0}^{N-1} \sin\frac{2\pi\cdot k(n-m)}{N} \tag{5}$$

after transformation of formula (3):

$$y_n = \frac{1}{N}\cdot\sum_{m=0}^{N-1}[y_m\cdot(A(n,m) + i\cdot B(n,m))] \tag{6}$$

Assuming that the vector $y_n$ is real, the equation (6) is true, when the imaginary part inside the sum is equal to zero.

### B. Resampling Errors

In order to compare the value of errors generated by algorithms specified in section IIA, four test signals with 1024 samples length have been defined:

- signal "A" containing frequencies from 0 Hz to $\frac{1}{3}f_{band}$ where $f_{band} = \frac{1}{2}\min(fs_{in}, fs_{out})$ and $fs_{in}, fs_{out}$ are input and output sampling frequency.
- signal "B" containing frequencies from $\frac{1}{3}f_{band}$ to $\frac{2}{3}f_{band}$
- signal "C" containing frequencies from $\frac{2}{3}f_{band}$ to $f_{band}$
- signal "D" containing frequencies from 0 Hz to $f_{band}$.

Frequency values, amplitudes and phases are random generated. Test signals A, B and C are generated as a superposition of 1000 sine waves and D contains 3000 sinusoids.

For the method of resampling by cascade of DA and AD, ideal converters are used. Interpolation and decimation resampling is performed with matlab "resample" function, which applies an antialiasing FIR lowpass filter.

Spectrum relative error of resampled signal is defined by formula (7):

$$\delta_Y = \frac{\sum_{n=0}^{N-1} ||Y_n| - |X_n||}{\sum_{n=0}^{N-1} |X_n|} \cdot 100\% \tag{7}$$

where $X_n, Y_n$ are DFT vectors of input and output signal used in resampling. The relative error of resampled signal in the time domain is defined by formula (8):

$$\delta_y = \frac{\sum_{n=0}^{N-1} |y_n - x_n|}{\sum_{n=0}^{N-1} |x_n|} \cdot 100\% \tag{8}$$

where $x_n, y_n$ are output signals vectors, respectively for ideal resampling and tested algorithm.

Upsampling ($fs_{in} = 44.1\,\text{kHz}, fs_{out} = 51.2\,\text{kHz}$) spectrum errors for all tested algorithms are shown in table I.

TABLE I
THE ERRORS OF UPSAMPLING OUTPUT SIGNALS SPECTRUM FOR ALL TESTED ALGORITHMS

| algorithm | signals A | B | C | D |
|---|---|---|---|---|
| linear interpolation | 4.2% | 26.4% | 61.1% | 30.4% |
| cascade of DA and AD | 25.1% | 61.8% | 98.6% | 40.5% |
| interpolation and decimation | 0.14% | 0.76% | 15.6% | 6.0% |
| spectral resampling | 0.11% | 0.82% | 2.9% | 0.91% |

In the context of harmonic analysis, the spectrum errors indicate which algorithm is most appropriate for signal optimization, but in general, in order to compare the resampling processing quality, deviations in the time domain are analysed. The values of time domain errors for upsampling are presented in table II.

The first two algorithms, optimized for high processing speed, generate significantly more distortions in comparison to the others, optimized for high quality. In addition, the higher signal frequencies, the lower processing quality can be observed for all algorithms.

The best results can be seen for spectral resampling which processes with the lowest errors for all frequencies (excluding medium). In this case, the influence of high frequencies is particularly low in comparison to the interpolation and decimation algorithm.

TABLE II
THE ERRORS OF UPSAMPLING OUTPUT SIGNALS FOR ALL TESTED ALGORITHMS

| algorithm | signals A | B | C | D |
|---|---|---|---|---|
| linear interpolation | 4.1% | 20.6% | 51.1% | 34.9% |
| cascade of DA and AD | 30.1% | 73.8% | 112% | 85.5% |
| interpolation and decimation | 0.05% | 0.11% | 23.7% | 14.2% |
| spectral resampling | 0.01% | 0.19% | 3.7% | 5.2% |

The quality tests was performed also for donwsampling ($fs_{in} = 44.1\,\text{kHz}, fs_{out} = 32.1\,\text{kHz}$). The errors of output signals spectrum are presented in table III.

TABLE III
THE ERRORS OF DOWNSAMPLING OUTPUT SIGNALS SPECTRUM FOR ALL TESTED ALGORITHMS

| algorithm | signals A | B | C | D |
|---|---|---|---|---|
| linear interpolation | 2.15% | 13.6% | 42.3% | 15.5% |
| cascade of DA and AD | 14.4% | 39.8% | 83.1% | 23.1% |
| interpolation and decimation | 1.03% | 1.89% | 9.62% | 3.19% |
| spectral resampling | 0.98% | 2.23% | 2.12% | 0.90% |

The values of time domain errors for downsampling are shown in table IV.

TABLE IV
THE ERRORS OF DOWNSAMPLING OUTPUT SIGNALS FOR ALL TESTED ALGORITHMS

| algorithm | signals A | B | C | D |
|---|---|---|---|---|
| linear interpolation | 2.28% | 11.9% | 28.9% | 17.6% |
| cascade of DA and AD | 21.9% | 55.5% | 89.6% | 62.2% |
| interpolation and decimation | 0.10% | 0.24% | 15.1% | 9.1% |
| spectral resampling | 0.11% | 0.83% | 2.58% | 1.8% |

The deviation distribution in frequency domain in case of signal "D" for both the most precise algorithms are presented in Fig. 5.

As it can be observed for the full bandwidth signal, the error values increase for high frequencies. The distribution of the absolute error values of signal "D" in a time domain for downsampling is shown in Fig. 6.

## III. USING THE SPECTRAL RESOLUTION OPTIMIZATION METHOD FOR REAL DIAGNOSTIC SIGNALS

Taking into consideration the quality of signal processing by algorithms presented in section II, to reduce the impact of resampling errors on the results of spectrum optimization, for all diagnostic signals, the spectral resolution adjustment is performed using a spectral resampling algorithm.

### A. Diagnostic Voice Acoustic Signal

To evaluate the progress of tongue rehabilitation, for example, after partial amputation, several recordings during the

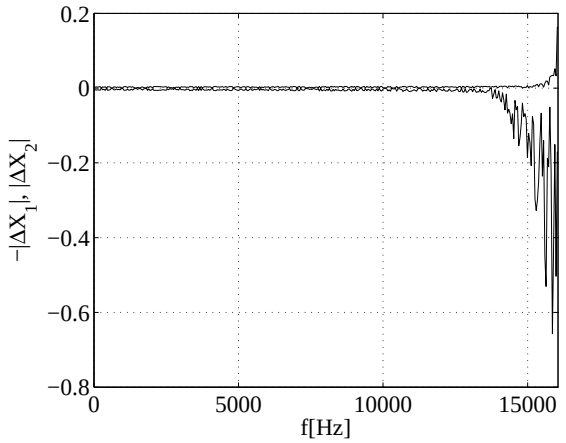


Fig. 5. The deviations distribution in frequency domain for signal "D" in case of downsampling. $\Delta X_1$, $\Delta X_2$ are deviations from ideal resampling of interpolation and decimation algorithm and spectral resampling

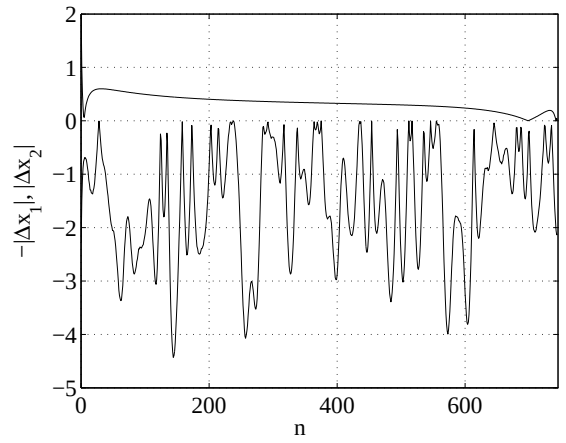


Fig. 6. The distribution of downsampling deviations in time domain for signal "D", $\Delta x_1$, $\Delta x_2$ are deviations from ideal resampling of output signals generated by interpolation and decimation algorithm and spectral resampling

process of rehabilitation are made for the patient pronouncing the same word [6]. Changes in the spectrum of the signals are analysed, in particular, the emergence of new harmonics [7]. The test diagnostic signal with the length of 2048 samples is a part of the first sound \ʌ\ of the recorded word \ʌdʌ\ pronounced by patient. In Fig. 7 the spectrum for the signal with native sampling frequency 44.1kHz is presented.

After changing sampling frequency to 60575Hz the spectral resolution is equal to 29.5Hz. The optimized signal spectrum is shown in Fig. 8.

### B. EEG signals

Frequency analysis of EEG signals is a very popular method of distinguishing between healthy and pathological cases [8]. In this approach, the leakage of the spectrum around harmonics can lead to incorrect conclusions. EEG signals contain only very low frequencies, so they are usually sampled with frequency around 200Hz. Fig. 9 shows Grass Technologies Comet with the AS40 amplifier, handling 19 channels, used for

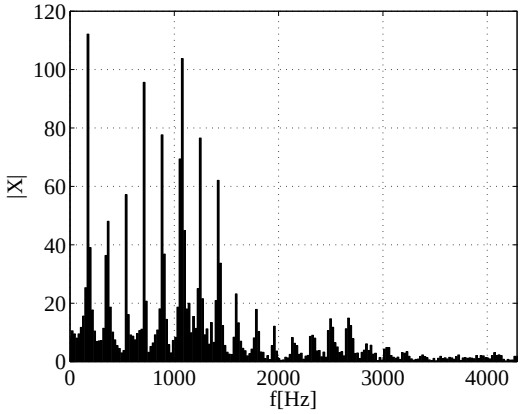


Fig. 7. Diagnostic signal spectrum of sound \ʌ\ pronunciation without any optimization

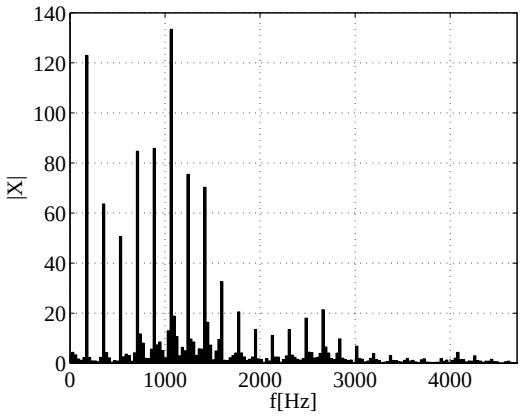


Fig. 8. Diagnostic signal spectrum of sound \ʌ\ pronunciation optimized by the adjustment of spectral resolution

the registration of the EEG test signal. During the recording, the patient is lying down.

The spectrum of the EEG signal from the Fp1-F4 channel, sampled at 200 Hz is shown in Fig. 10. The signal length is 1024 samples.

Fig. 11. shows the spectrum of the EEG signal after adjusting the spectral resolution to 0.2028Hz.

### C. Vibroacoustic Signals In The Diagnostics Of Transformers

To evaluate the mechanical state of the active part of the high power transformer, spectrum of the vibration signal of the transformer tank can be analysed. In the steady state, foreign frequencies around harmonics, which are multiples of 50Hz indicate some faults [9]. There are two transformers tested, whose tank vibration are analysed: TONa 800/15 0.8 MVA presented in Fig. 12 and TDRbz-25000/110 25MVA. For both transformers, the vibrations are recorded digitally using SVAN958 with a sampling rate of 48 kHz, without load. The length of both test signals is 4096 samples. The main difference between signals is the fundamental frequency. For a 25MVA transformer, it is 200Hz, for 0.8MVA 100Hz

The native spectrum of 0.8 MVA transformer is presented in Fig. 13 and for 25MVA in Fig. 14. The spectrum after

Fig. 9. Grass Technologies Comet with AS40 amplifier used to record the EEG signal

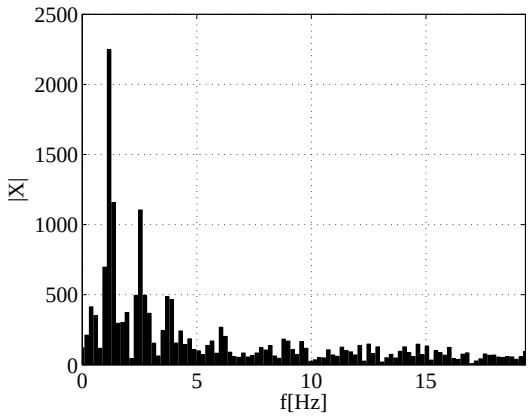


Fig. 10. The spectrum of the EEG signal without any optimization

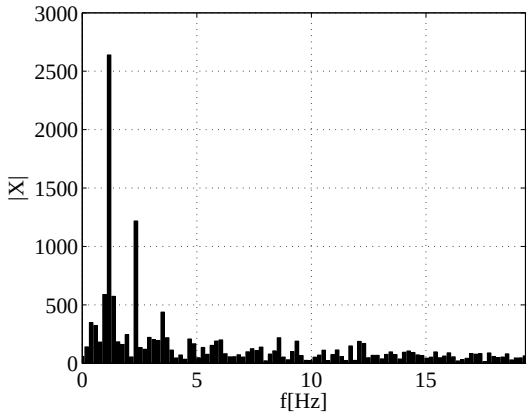


Fig. 11. The spectrum of the EEG signal optimized by the adjustment of spectral resolution

optimization by resampling to 102.4kHz is shown in Fig. 15 for 0.8 MVA transformer and in Fig. 16 for 25MVA.

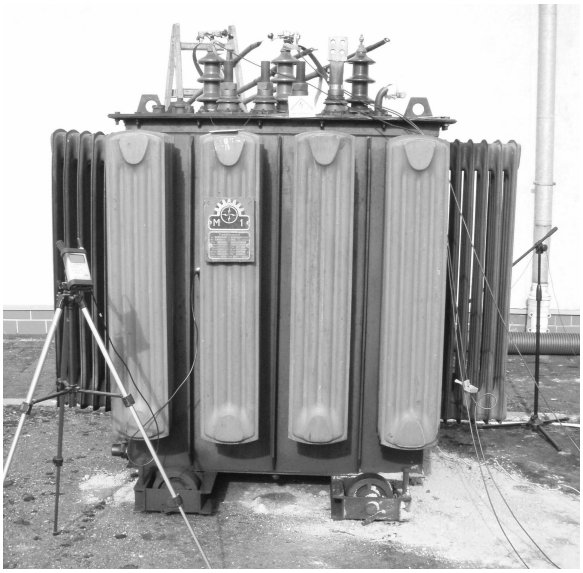

Fig. 12. Transformer TONa 800/15 0.8 MVA during recording of the tank vibration signal

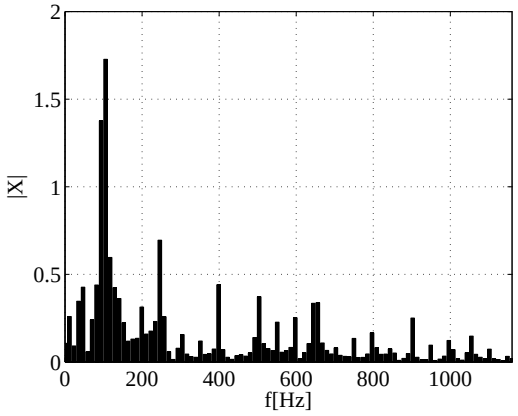


Fig. 13. The spectrum of the vibroacustic signal of the transformer tank without any optimization for TONa 800/15

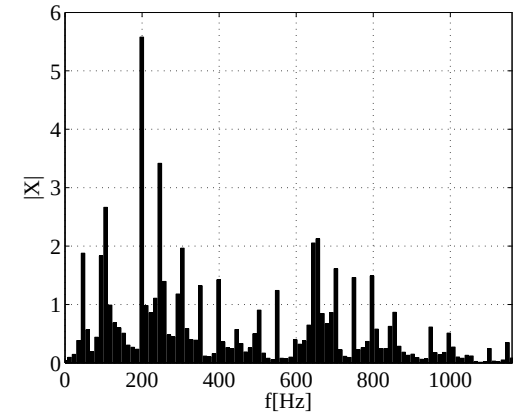


Fig. 14. The spectrum of the vibroacustic signal of the transformer tank without any optimization for TDRbz-25000/110

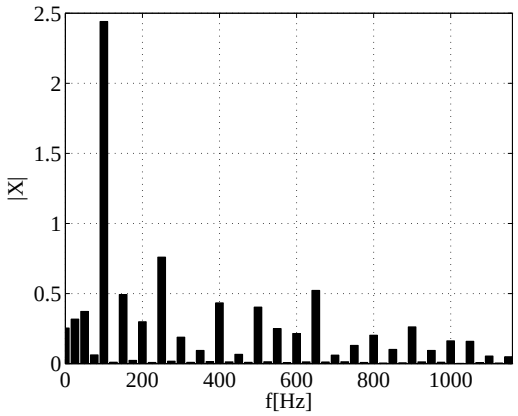


Fig. 15. The spectrum of the vibroacustic signal of the transformer tank optimized by the adjustments of spectral resolution for TONa 800/15

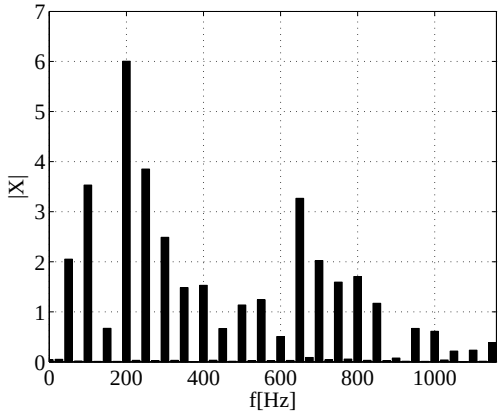


Fig. 16. The spectrum of the vibroacustic signal of the transformer tank optimized by the adjustments of spectral resolution for TDRbz-25000/110

### *D. Acoustic Signal Of The Car Engine Operation*

The spectrum of sound produced by the car engine can be used for diagnostic purposes, but its structure is more complicated than in the case of transformers [10]. It is due to the noise caused by valves, camshafts, oil pumps, etc. The test signal was registered by the microphone as shown in Fig. 17.

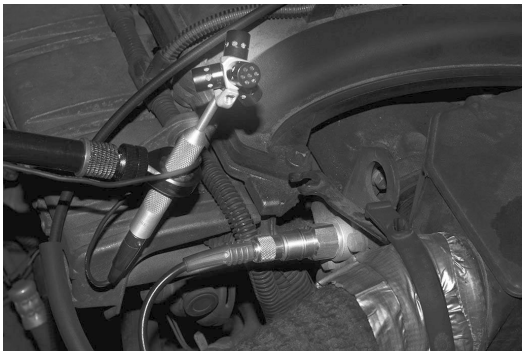

Fig. 17. Microphone recording an acoustic signal of the car engine operation

The number of cylinders of the tested engine is 4, the displacement 1.6 liters, the number of valves is 16.

The signal can only be optimized for the main harmonics related to the engine's ignition period. The low part of the spectrum with harmonics and noise without optimization is presented in Fig. 18. The signal length is 8192 samples and a native sampling rate is 48kHz. The spectrum after optimization by resampling to 48575Hz is shown in Figure 19.

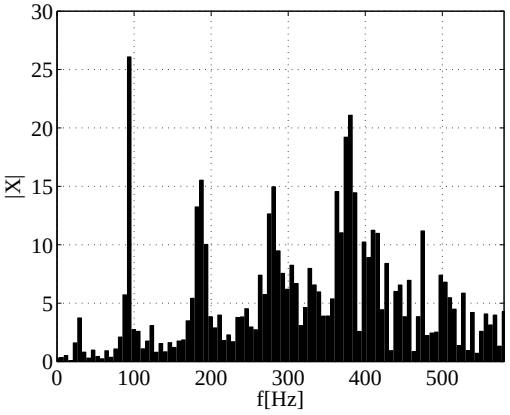


Fig. 18. The spectrum of the car engine's acoustic signal without any optimization

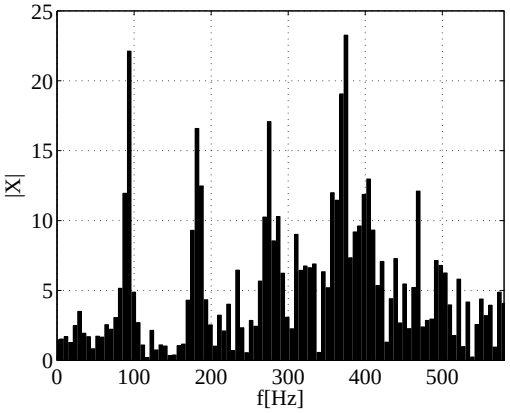


Fig. 19. The spectrum of the car engine's acoustic signal optimized by the adjustments of spectral resolution

### *E. Acoustic Signal Of The Car Engine Exhaust Gas*

The acoustic signal of the car engine exhaust gas can be used for the diagnostics of an ignition process and combustion of the fuel mixture [11]. The noise level is significantly lower than in the case of the car engine sound recorded directly by the microphone, so the spectrum optimization effects are better. Test signal is recorded for the engine running at idle and its unoptimized spectrum is shown in Fig. 20.

The digital recording is performed with 44.1kHz sampling frequency, and the spectrum is computed for 2048 samples. For the optimization purposes, the signal is resampled to 69632Hz and after this operation the spectral resolution is 340Hz. The spectrum of the test signal after adjustments of the spectral resolution is presented in Fig. 21.

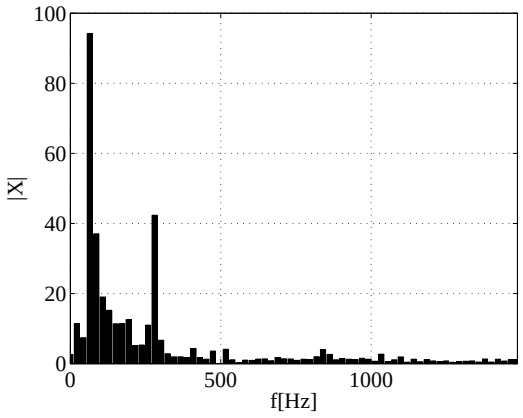


Fig. 20. The spectrum of the acoustic signal of the car engine exhaust gas without any optimization

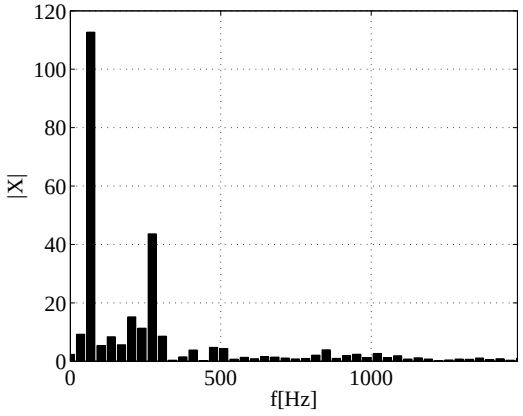


Fig. 21. The spectrum of the acoustic signal of the car engine exhaust gas optimized by the adjustments of spectral resolution

## IV. Conclusion

The use of resampling to improve harmonic analysis introduces additional distortions to the signal that can be observed in the spectrum. For this reason, only high-quality resampling algorithms should be used for this purpose. As a result of comparing the four algorithms, spectral resampling has been chosen. This algorithm, in both time and frequency domain, generates the lowest error values excluding signals containing only medium frequencies. However, in this case the errors are only insignificantly higher than in the case of the interpolation and decimation algorithm.

Tests performed for the real diagnostic signals prove the effectiveness of the method. For a simple spectral structure (voice acoustic signal, vibroacoustic signals of transformers, acoustic signal of car exhausts), as a result of optimization, a clear spectrum is obtained (harmonics and low level noise). Then, discovering the foreign frequencies is simple and unambiguous. The EEG signal and the sound of the car engine operation have a more complex spectral structure, so discovering foreign frequencies is generally problematic. For this reason, the main goal for such signals is to obtain the proper values of harmonic parameters. Then, it is possible to analyse correctly the relations between harmonics or discover low amplitude harmonics.

## References

[1] R. G. Lyons, *Understanding digital signal processing*, New Jersey, USA: Prentice Hall 2010

[2] S. J. Orfanidis, *Introduction to signal processing*, Upper Saddle River, USA: Prentice Hall 2010

[3] D. Borkowski, R. Dlugosz, M. Szulc and, P. Skruch, *Multi-Rate Signal Processing Issues in Active Safety Algorithms*, SAE Technical Paper, 2016

[4] A. Muhammad, *On the implementation of integer and non-integer sampling rate conversion*, Linköping, Sweden: Linköping University Electronic Press, 2012

[5] M. Jarmołowicz and E. Kornatowski, *Method of vibroacoustic signal spectrum optimization in diagnostics of devices*, 2017 International Conference on Systems, Signals and Image Processing (IWSSIP), IEEE Xplore, 2017

[6] V. Parsa and D. G. Jamieson, *Acoustic Discrimination of Pathological Voice*, Journal of Speech, Language, and Hearing Research, 2001

[7] J. Laaksonen, I. J. Loewen, J. Wolfaardt, J. Rieger, H. Seikaly and J. Harr, *Speech After Tongue Reconstruction and Use of a Palatal Augmentation Prosthesis: An acoustic case study*, Ottawa, Canada: Canadian Journal of Speech-Language Pathology and Audiology, 2009

[8] S. Sanei and J. Chambers, *EEG signal processing*, Cardiff University, England: John Wiley & Sons, Inc., 2007

[9] E. Kornatowski, *Mechanical-condition assessment of power transformer using vibroacoustic analysis*, Key Engineering Materials 2012

[10] W. Li, F. Gu, D. A. Ball, A. Y. T. Leung and C. E. Phipps, *A study of the noise from diesel engines using the independent component analysis*, Mechanical Systems and Signal Processing 2001

[11] L. Barelli, G. Bidini, C. Buratti, R. Mariani, *Diagnosis of internal combustion engine through vibration and acoustic pressure non-intrusive measurements*, Applied Thermal Engineering 2009